Journal of Power Sources 230 (2013) 70–75

Contents lists available at SciVerse ScienceDirect

Journal of Power Sources

journal homepage: www.elsevier.com/locate/jpowsour

# Production of $Cu_2(Zn,Fe)SnS_4$ powders for thin film solar cell by high energy ball milling

C.L. Azanza Ricardo [a,*], M.S. Su'ait [a,b], M. Müller [a,c], P. Scardi [a]

[a] Department of Civil, Environmental and Mechanical Engineering, University of Trento, via Mesiano 77, 38123 Trento, Italy
[b] School of Chemical Sciences and Food Technology, Faculty of Science and Technology, University Kebangsaan Malaysia, 43600 Bangi, Selangor, Malaysia
[c] Max Planck Institute for Solid State Research, Heisenbergstr. 1, 70569 Stuttgart, Germany

## HIGHLIGHTS

- $Cu_2(Zn,Fe)SnS_4$ powders were successfully produced using high energy ball milling.
- Iron substitution in the Zn site of the kesterite structure, was studied.
- XPS measurements revealed the proper oxidation state of iron.
- In-situ SXRD was used to follow the system evolution into final CZTS structure.
- Solar-inks were successfully obtained and deposited via spin-coating technique.

## ARTICLE INFO

*Article history:*
Received 23 August 2012
Received in revised form
24 October 2012
Accepted 9 December 2012
Available online 20 December 2012

*Keywords:*
Ball-milling
CZTS
XRD
Solar-ink

## ABSTRACT

Copper zinc tin sulfide ($Cu_2ZnSnS_4$, CZTS) is nowadays one of the most promising materials as an alternative to the well known absorber in the CIGS thin film solar cells. Additionally to the non toxicity of the single species; the material suitable bandgap and large absorption coefficient, low-cost and large-area deposition techniques are already under development in order to avoid expensive vacuum-based processes. In this work high energy ball milling was used to obtain $Cu_2(Zn,Fe)SnS_4$ powders for solar-inks production. Optimal conditions for the milling and for the following annealing process are described in detail. Substitution of zinc by iron, either as an effect of contamination from the milling vials and/or as an addition in controlled quantity, was studied by structural (XRD) and chemical (SEM-EDX) techniques. XPS measurements provided further information on the oxidation state of iron, whereas in-situ high temperature synchrotron radiation XRD was used to follow the evolution of the system, and in particular the transformation of iron from the starting metallic condition to the alloying in the final kesterite powders.



## 1. Introduction

Nowadays, thin film solar cells based on CIGS ($CuIn_{1-x}Ga_xSe_2$ with $x \sim 0.3$) heterojunctions show record efficiency of 20.3% [1]. However, alternative solutions not employing expensive or toxic species such as In, Ga, Te or Cd, and using materials with attractive physical properties are the object of many studies. Chalcogenide compounds with stoichiometry $Cu_2(MII)(MIV)(S,Se)_4$ (MII = Mn, Fe, Co, Ni, Zn, Cd, Hg and MIV = Si, Ge, Sn) have drawn attention in recent past, because of abundance of the starting mineral phases, based on environment-friendly non-toxic materials (with the exception of expensive and potentially toxic elements such as Cd, Hg and Ge) and also for the direct bandgap, most suited to applications in solar cells and other optical devices [2].

Kesterite (space group $I\bar{4}$) and stannite (space group $I\bar{4}2$ m) have a crystal structure similar to that of chalcopyrite, with just a different arrangement of Cu and Zn atoms [2–5]. The similarity to the crystal structure of CIGS makes this class of quaternary chalcogenides the object of extensive research: in particular, $Cu_2ZnSnS_4$ (CZTS) is one of the best candidates as absorber layer material in low-cost thin film solar cells, with a direct bandgap of ~1.5 eV and a large optical absorption coefficient ($>10^4$ $cm^{-1}$). Preliminary results on non-optimized thin film solar cells based on CZTS already reached a 8.4% efficiency [6].

Among the possible material improvements, the substitution of zinc atoms with iron in chalcogenide compounds is an open and

* Corresponding author. DICAM, University of Trento, via Mesiano 77, 38123 Trento, Italy. Tel.: +39 0461282477.
*E-mail address:* Cristy.Azanza@ing.unitn.it (C.L. Azanza Ricardo).

0378-7753/$ – see front matter © 2012 Elsevier B.V. All rights reserved.
http://dx.doi.org/10.1016/j.jpowsour.2012.12.045

promising research field. Besides possible effects on the performance of kesterite as an absorber layer, investigations are further motivated by the occurrence of zinc-iron substitution in the natural kesterite structure $Cu_2(Zn,Fe)SnS_4$ [7].

Several studies on the use of mechanical milling for CZTS production and ink deposition are available [8–10]. In a recent work [8] milling in agata vials was used for mixing the starting powders, and as a last stage for reducing grain dimensions. Other works [10] were based on planetary ball milling, to obtain single-phase CZTS precursor powders. The milling process can also be used to grind precursor powders down to nanosize, to obtain a homogeneous and well-dispersed slurry [9].

In order to prepare solar inks, the precursor powders should be finely dispersed in the solvent. However, the use of toxic and/or unstable compounds, like in hydrazine-based slurry, seems not a viable solution in view of a large-scale solar cell fabrication, even if it may lead to high efficiencies [11]. Successful results have been reported using ethanol as a non-toxic solvent [9], leading to the fabrication of dense CZTS absorber layers granting a 5.14% efficiency in thin film solar cells. In addition, solar inks based on ethanol can evaporate quickly, and minimize residual carbon or oxygen impurities [9].

CZTS thin film deposition techniques can be classified into two broad categories: vacuum, and non-vacuum based methods [12]. Vacuum-based fabrication techniques normally involve deposition of the basic components of CZTS on a substrate by sputtering [13], evaporation [14] or co-evaporation [15] of the target sources under a certain pressure and temperature. These techniques have the advantage of easily controlling chemical composition and phase profile, and normally provide a good reproducibility. Among the possible drawbacks, one should consider the relatively slow throughput, low material utilization, high costs, including energy consumption, and difficulty in the scale-up to commercial production level [9,10,12]. Non-vacuum based deposition techniques, on the contrary, should involve low production costs as a major advantage. For this reason methods like spin coating [11,16], screen printing [8,10], electrochemical deposition [17], and spray pyrolysis [18] of precursor solutions have been widely investigated for the preparation of semiconductor thin films.

Combining the low cost of starting materials and their non-toxicity with a low cost production technology like ball-milling, and a very simple deposition method like spin coating using particle suspensions (inks), seems a promising solution. In this work, CZTS particles were prepared by high energy planetary milling and were deposited by spin coating via ink solution. Obtained powders were thermally treated and characterized by XRD and SEM-EDAX. XPS and high temperature in-situ XRD synchrotron measurements were used for a better understanding of the evolution and behavior of the introduced jar contamination.

## 2. Experimental

Starting materials for CZTS precursor, Cu powder (<75 μm, 99%), Zn powder (purum, 99%), Fe fine powder (99%), Sn powder (puriss, 99%) and Sulfur flakes (purum, 99.5%) were purchased from Sigma–Aldrich (St. Louis, MO, USA). Ethanol (99.8%) was supplied by Fluka Analytical (Sigma–Aldrich, St. Louis, MO, USA). For ink production, α-terpineol (96%) purchased from SAFC (Sigma–Aldrich, St. Louis, MO, USA) and ethyl cellulose by Sigma–Aldrich (St. Louis, MO, USA) were used.

$Cu_2(Zn_{1-x}, Fe_x)SnS_4$($x$ = 0.0–1.0) in stoichiometric ratio of ($2{:}x{:}1-x{:}1{:}4$) was prepared by milling, using 250 μL ethanol as lubricant. The milling of the precursor powder was performed by a P4 planetary milling (Fritsch Pulverisette 4) (Fritsch GmbH, Idar-Oberstein, Germany), using 80 mL stainless steel bowls (AISI304) and 25 balls made of tempered 100Cr6 steel (12 mm in diameter). High energy milling conditions were used: relative ratio between revolution speed of the planets ($\omega$ = 540 rpm) and speed of main disk ($\sigma$ = 300 rpm) was fixed to $\omega/\sigma = -1.8$ [19,20]. Precursor powders were then annealed under Argon flux at 550 °C for 2 h with the presence of sulfur atmosphere to promote complete formation of a CZTS powder.

Ink solutions were prepared by the method proposed by [10]. The solutions were deposited on glass substrates by spin coating using a rotational speed of 800 rpm for 60 s, and were dried at 200 °C for 5 min in air. The spin coating and drying processes were repeated several times to obtain the desired thickness.

X-ray diffraction (XRD) laboratory measurements were performed on standard laboratory instruments. For the powders analysis a THERMO diffractometer with Mo radiation was used in standard Bragg–Brentano geometry, whereas for thin film characterization an X'Pert PANAlytical instrument was used in grazing incidence configuration. Energy-dispersive X-ray spectroscopy (EDX) was performed for controlling sample stoichiometry, using a Philips XL30 ESEM with an EDAX detector. X-ray photoelectron spectroscopy (XPS) measurements, carried out to check oxidation states of the species of interest, were made on a Scienta ESCA 200 with a monocromatic AlKα radiation.

High temperature in-situ XRD synchrotron radiation measurements were performed on the MCX beamline at Elettra (Trieste), the Italian synchrotron radiation facility. Quartz capillaries of 0.5 mm diameter with a localized heating system (hot air blower) were used. X-ray energy was 15 keV.

## 3. Results and discussion

Several milling conditions like milling time, speed and/or milling mechanism (i.e. planetary mill or vibrational mill), weight ratio between starting powder and milling balls, as well as lubricant amount (ethanol, in the present case) were prelimarily optimized. In order to induce a reaction of the starting powders during the milling process, steel vials and balls were used. The best compromise between milling efficiency and vial damaging or introduced contamination was found to be the following: 3 h milling time with a weight ratio of 100:1 and ethanol volume of 250 μL. All samples showed CZTS with small crystalline domain size (large diffraction peaks) together with a significant amount of unmilled Sn and Zn. Fig. 1 (left) shows the XRD profiles (collected with Mo radiation) of a set of as-milled samples, where it is possible to notice the increasing amount of unmilled material, correlated with the progressive milling process. This effect originates from the increasing wear of the steel jars. In order to overcome this problem, to complete CZTS formation and to increase the grains dimensions, a further step of heat treatment was optimized, leading to fully CZTS powders. This annealing step was performed under Ar flux and sulfur atmosphere at 550 °C for 2 h. Fig. 1 (right) shows the effect of the heat treatment on one of the last produced samples (27 in left figure) giving no traces of metallic residuals.

SEM-EDAX measurements performed to control sample composition gave a constant iron contamination from jars, of the order of 0.5 in atomic ratio (corresponding to a 5% in atomic weight). Even if metallic iron is not visible in the XRD patterns of the heat treated samples, XPS spectroscopy was used to determine the chemical and electronic state of the elements present on the surface of the CZTS powders. For these measurement one sample was chosen after the recrystallization heat treatment was performed. Fig. 2 shows the core-level spectrum of Cu 2p, Zn 2p, Fe 2p, Fe 3p, Sn 3d and S 2p levels. The results showed the characteristic peaks for $Cu^+$ (peaks at 931.9 eV and 951.7 eV with a peak separation of 19.0 eV for the Cu 2p), $Zn^{2+}$ (peaks at 1022.0 eV and

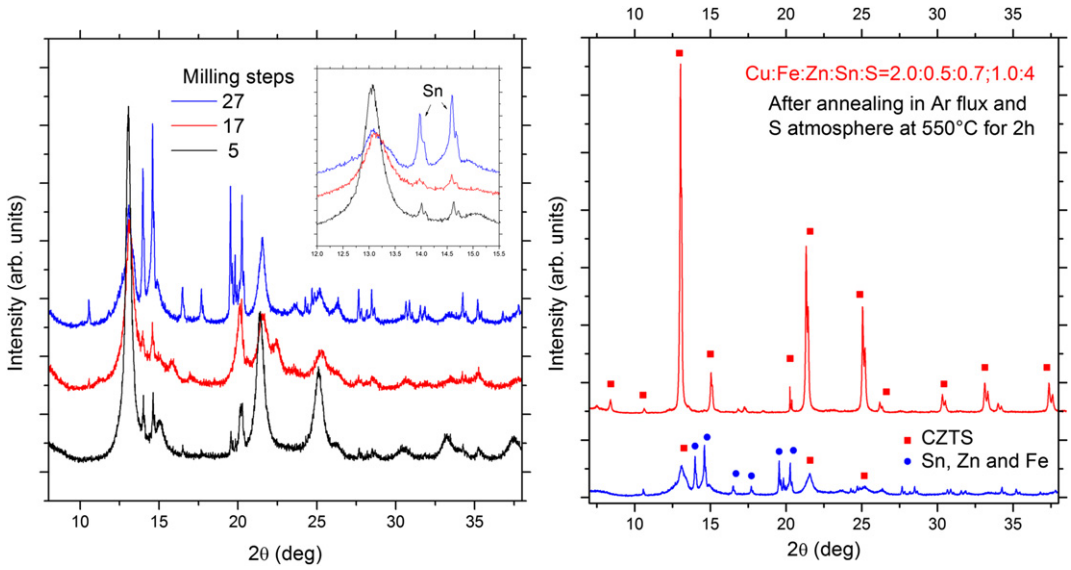


**Fig. 1.** Effect of the progressive milling (left) and heat treatment on the as milled powders (right).

1045.1 eV with a peak separation of 23.1 eV for the Zn 2p), $Sn^{4+}$ (peaks at 486.3 eV and 494.9 eV with a peak separation of 8.6 eV for the Sn 3d) and $S^{2-}$ (peaks at 161.5 eV and 162.0 eV with a peak splitting of 1.1 eV for the S 2p), in agreement with what reported by the literature on this material [21]. The presence of the binding energy signal at 168.9 eV for S 2p level is a fingerprint of sulfate phases, most likely coming from chemisorption of oxygen on the particle surface [22]. An important result is the complete absence of the metallic iron signal Fe(0) in the measurement of the 2p core level. However, due to the superposition with other signals in the same binding energy region, it was not possible to fully identify the Fe(II) peak. As an alternative, the Fe 3p level was measured, showing the Fe(II) signal at 56.0 eV. It is therefore possible to conclude that no metallic iron, coming from steel jar contamination, is present in the produced samples after performing the heat treatment.

For the study of the phase evolution (i.e. incorporation of the residual metallic unmilled powder into the kesterite structure) and the recrystallization kinetics during the thermal treatment, in-situ high temperature XRD Synchrotron radiation XRD (SRXRD) was

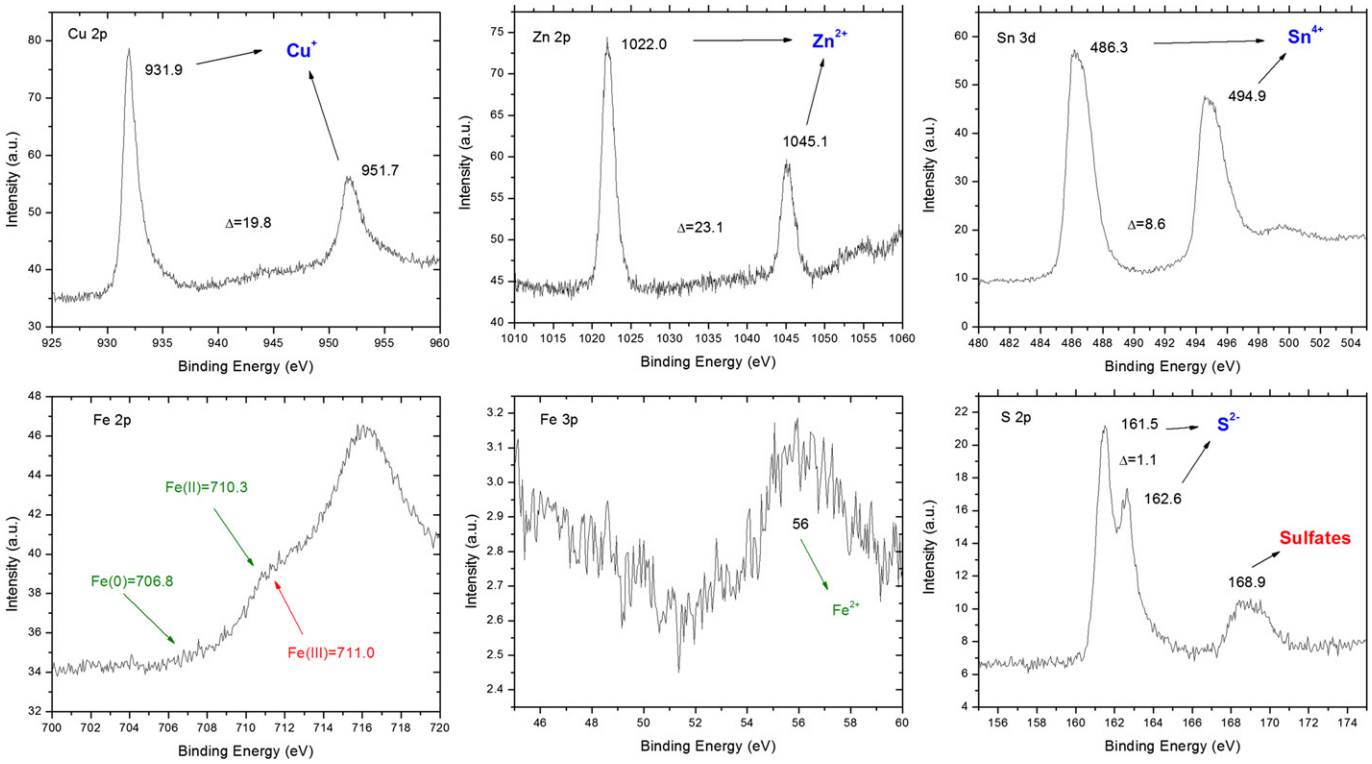


**Fig. 2.** XPS measurements for the Cu 2p, Zn 2p, Sn 3d, Fe 2p, Fe 3p and S 2p levels.

performed [23] on the MCX beamline at Elettra, the Italian synchrotron radiation facility in Trieste. With this technique, it is possible to use a small amount of powder and perform fast measurements. Two set of measurements are shown in this work, using a 0.5 mm quartz capillary with a localized heating system (hot air blower) in one case, whereas an oven with an imaging plate was used for a second set of measurements. In both cases the beam energy was set to 15 keV in order to avoid absorption edges of the starting materials. Using high energies (i.e. lower wavelengths) also increases the number of collected reflections in a short time measurement.

Fig. 3 shows measured profiles for each selected temperature (left) together with the line profile analysis results (right) for two samples: (i) is one of the first milling steps, labeled as number 5 in Fig. 1 (up), whereas (ii) is a sample after several milling steps, labeled as number 27 in the same figure (down). Using the information obtained from the profile analysis, it is possible to identify three main regions in both cases:

- below 300 °C the average crystalline domain size remains almost the same, while the Sn, Zn and Fe amounts keep decreasing due to the formation of zinc sulfides (ZnS) and tin

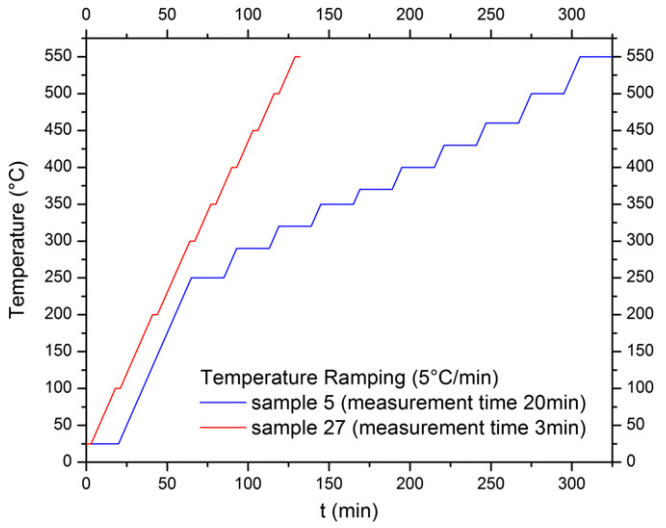


**Fig. 4.** Temperature ramping for the standard measurement with the hot air blower and with the oven with imaging plate.

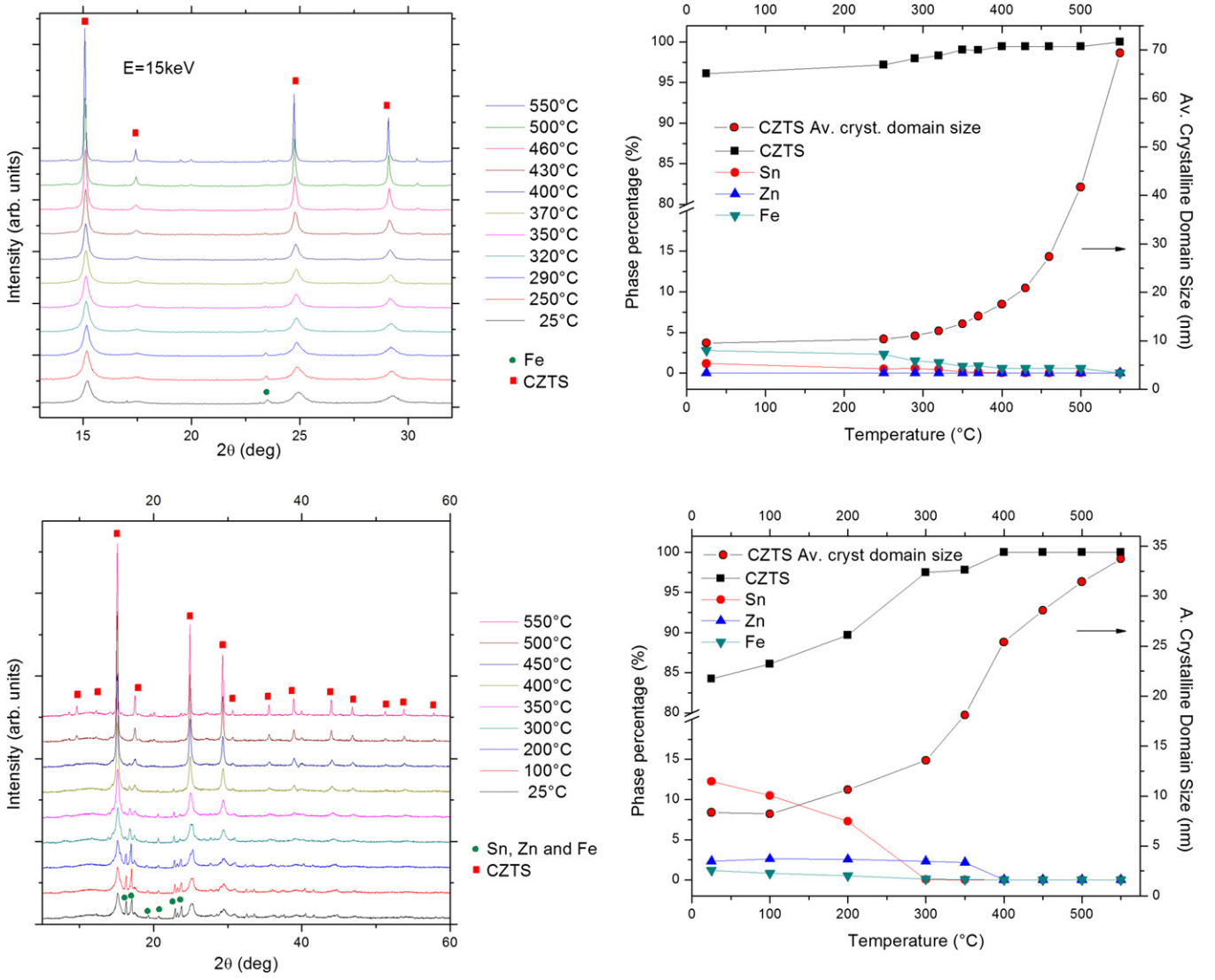


**Fig. 3.** XRD measurements and line profile analysis results.

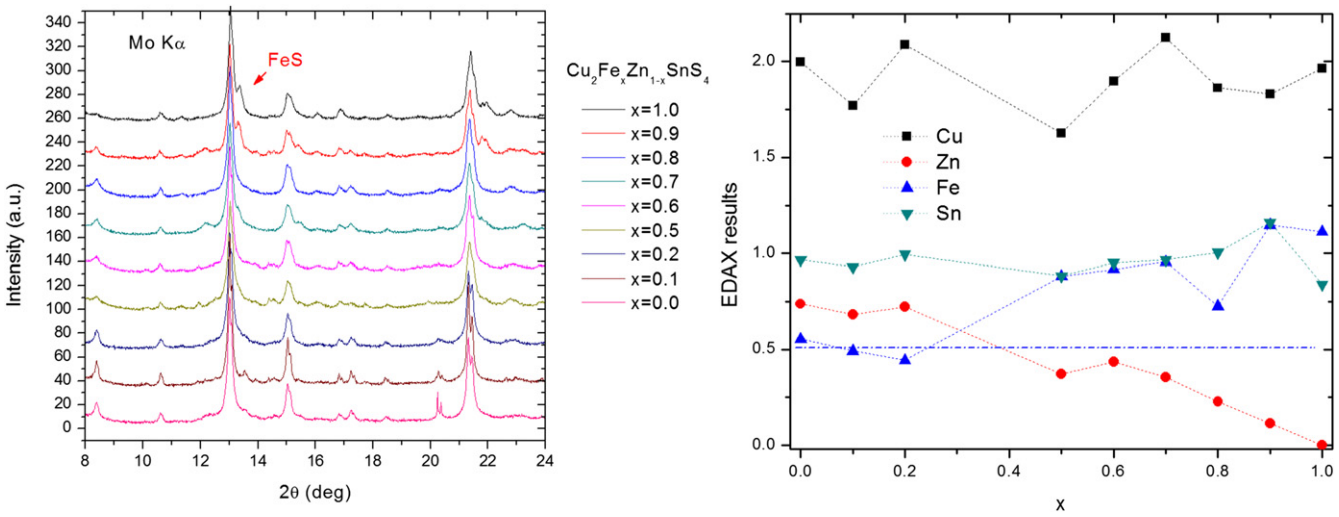


**Fig. 5.** XRD measurements and EDX results trend for the produced powders.

sulfides ($SnS_2$) [24,25]. The process starts when S diffuses into the precursor powders to react with the metallic elements. The first binary sulfides such as copper sulfides ($Cu_{2-x}S$, $0 \leq x \leq 1$), ZnS and $SnS_2$ are formed after pre-heating below temperatures of 300–350 °C;

- between 300 °C and 550 °C the recrystallization effect is quite evident. Sulfides react with the excess sulfur to form more complex structures like $Cu_2SnS_3$. However, there is still a small amount of metallic Sn and/or Zn;
- using higher temperatures samples are fully crystallized and the starting materials are completely incorporated into the kesterite structure. Further increasing the temperature leads to minor differences. For example, small amounts of $SnO_2$ can be found most likely due to the formation of small cracks in the quartz capillary altering the working atmosphere [26].

Main differences between performed measurements are related to the recrystallization growth and are a direct consequence of the different temperature ramping used in the two different measurement setup. Fig. 4 shows in detail that for a standard measurement more time is necessary to collect a useful $2\theta$-range (20 min) with respect to the 3 min used with the imaging plate to collect a whole $2\theta$-range. Therefore, even if the recrystallization trend is almost the same in both cases, in the former condition the sample is exposed for a longer time to high temperatures and thus the crystalline domain size at the end of the experiment is larger than when using the imaging plate.

In order to further study the solubility of Fe in the kesterite structure, controlled amounts of iron were added as starting material leading to a composition $Cu_2Fe_xZn_{1-x}SnS_4$ (with $0 \leq x \leq 1$). SEM-EDAX measurements together with standard laboratory XRD measurements were performed for each sample after the annealing step, to following the structural and compositional evolution of the produced powders as a function of the added Fe content.

From XRD measurements it can be noticed that above 0.7 in atomic ratio some features on the left side of the CZTS diffraction peaks are observed. This signal was identified as that of FeS, whose presence is a consequence of the iron excess. In fact, as stated before, standard samples (i.e. without additional iron) already showed about 0.5 atomic ratio of iron, which corresponds to the lower limit detected for all measured samples (Fig. 5 right). In fact,

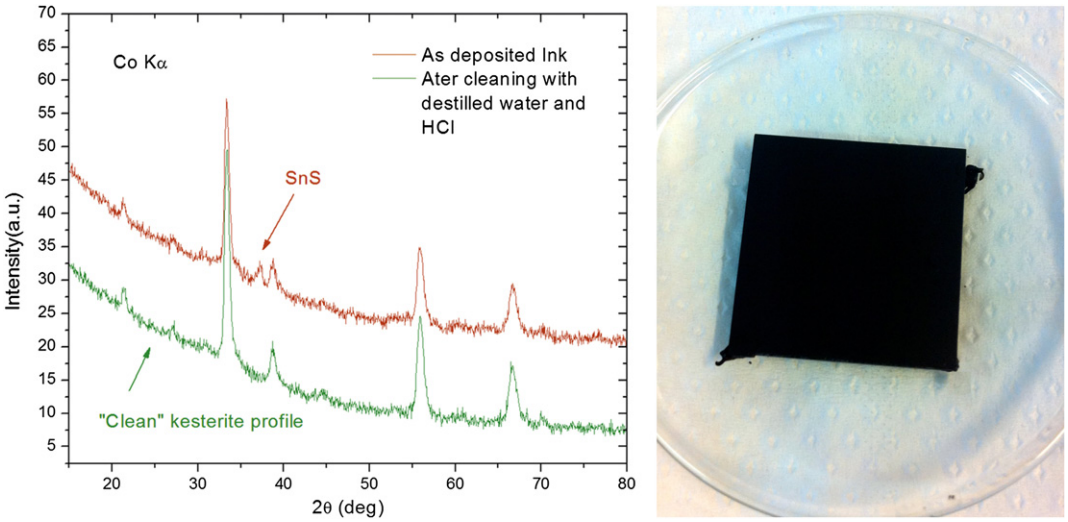


**Fig. 6.** XRD measurements of the deposited ink before and after HCl cleaning.

it is possible to notice that Zn content gives a decreasing linear trend while Fe content increases for $x$ values above 0.5.

After the recrystallization heat treatment the obtained powders were used to produce a CZTS ink based on $\alpha$-terpinol and cellulose for stabilization and polymerization in an ethanol-based solution [10]. The inks can be easily deposited by spin-coating, followed by a further annealing step for the evaporation of the organic compounds. Fig. 6 (right) shows the final CZTS layer deposited on a glass substrate (thickness of about 2 μm roughness around 0.02 μm), together with the grazing incidence XRD pattern of the as deposited layer (left) and after cleaning with HCl (right). This cleaning step is often proposed in literature [27] for removing spurious phases. In our case it seems appropriate to remove some residual SnS, as clearly shown by the XRD patterns. Even if this phase was not detected in the starting powders its formation could be related to the heat treatment performed for removing ink organic compounds.

## 4. Conclusions

High energy ball-milled CZTS powders were produced from metallic precursors and studied in detail. The production process as well as the recrystallization thermal treatment were fully optimized leading to fully kesterite samples with different levels of iron contamination from the milling vials. The oxidation state of iron studied by XPS showed no traces of metallic iron in the final semiconductor phase. Structure and microstructure of the CZTS phase was studied by XRD, with in-situ high temperature SRXRD measurements to follow up its evolution during heat treatment. CZTS ink was used together with the spin-coating deposition technique to produce thin films made of nanocrystalline grains. Preliminary results related to the effect of the introduction of iron in controlled amounts are presented. A lower limit in the iron content was found (about 0.5 atomic ratio), fully compatible with microanalysis results for samples without additional Fe.

## Acknowledgments

Authors would like to thank all the MCX beamline staff of the Elettra Synchrotron Radiation Facility at Trieste, and in particular Dr. Andrea Lausi and Dr. Jasper Plasier. Special thanks to Dr. Lia Vanzetti for the XPS measurements and useful discussion.

## References

[1] P. Jackson, D. Hariskos, E. Lotter, S. Paetel, R. Wuerz, R. Menner, W. Wischmann, M. Powall, Prog. Photovolt Res. Appl. 19 (2011) 894–897.
[2] D.B. Mitzi, O. Gunawan, T.K. Todorov, K. Wang, S. Guha, Sol. Energy Mater. Sol. Cells 95 (2011) 1421–1436.
[3] S. Siebentritt, S. Schorr, Prog. Photovolt Res. Appl. (2012).
[4] S. Chen, W.-J. Yin, J.-H. Yang, X.G. Gong, A. Walsh, S.-H. Wei, Appl. Phys. Lett. 95 (2009) 052102.
[5] S. Chen, X.G. Gong, Phys. Rev. B 79 (2009) 165211.
[6] B. Shin, O. Gunawan, Y. Zhu, N.A. Bojarczuk, S.J. Chey, S. Guha, Prog. Photovolt Res. Appl. (2011).
[7] S. Hall, J. Szymanski, J. Stewart, Can. Mineral. 16 (1978) 131–137.
[8] Z. Zhou, Y. Wang, D. Xu, Y. Zhang, Sol. Energy Mater. Sol. Cells 94 (2010) 2042–2045.
[9] K. Woo, Y. Kim, J. Moon, Energy Environ. Sci. 5 (2012) 5340–5345.
[10] Q. Chen, X. Dou, Z. Li, S. Cheng, S. Zhuang, Adv. Mater. Res. 335-336 (2011) 1406–1411.
[11] T.K. Todorov, K.B. Reuter, D.B. Mitzi, Adv. Mater. 22 (2010) E156–E159.
[12] H. Wang, Int. J. Photoenergy 2011 (2011). 10 pages.
[13] J.-S. Seol, S.-Y. Lee, J.-C. Lee, H.-D. Nam, K.-H. Kim, Sol. Energy Mater. Sol. Cells 75 (2003) 155–162.
[14] C. Shi, G. Shi, Z. Chen, P. Yang, M. Yao, Mater. Lett. 73 (2012) 89–91.
[15] T. Tanaka, D. Kawasaki, M. Nishio, Q. Guo, H. Ogawa, Phys. Status Solidi C 3 (2006) 2844–2847.
[16] K. Tanaka, M. Oonuki, N. Moritake, H. Uchiki, Sol. Energy Mater. Sol. Cells 93 (2009) 583–587.
[17] C. Chan, H. Lam, C. Surya, Sol. Energy Mater. Sol. Cells 94 (2010) 207–211.
[18] V. Rajeshmon, C.S. Kartha, K. Vijayakumar, C. Sanjeeviraja, T. Abe, Y. Kashiwaba, Sol. Energy 85 (2011) 249–255.
[19] M. Leoni, P. Scardi, M. D'Incau, G. Luciani, Metall. Mater. Trans. A (2011) 1–6.
[20] M. D'Incau, M. Leoni, P. Scardi, J. Mater. Res. 22 (6) (2007) 1744–1753.
[21] M. Cao, Y. Shena, J. Cryst. Growth 318 (2011) 1117–1120.
[22] M. Bouaziz, K. Boubaker, M. Amlouk, S. Belgacem, J. Phase Equilib. Diffus. 1547-7037 (2010).
[23] S. Schorr, A. Weber, V. Honkimki, H.-W. Schock, Thin Solid Films 517 (2009) 2461–2464.
[24] C. Platzer-Björkman, J. Scragg, H. Flammersberger, T. Kubart, M. Edoff, Sol. Energy Mater. Sol. Cells 98 (2012) 110–117.
[25] J.J. Scragg, Studies of $Cu_2ZnSnS_4$ films prepared by sulfurisation of electrodeposited precursors, Ph.D. thesis, Department of Chemistry, University of Bath, 2010.
[26] B. Pawar, S. Pawar, K. Gurav, S. Shin, J. Lee, S. Kolekar, J. Kim, ISRN Renew. Energy 2011 (2011).
[27] K. Maeda, K. Tanaka, Y. Fukui, H. Uchiki, Sol. Energy Mater. Sol. Cells 95 (2011) 2855–2860.